Soldering of Carbon Materials Using Transition Metal Rich Alloys

Marek Burda,*,† Agnieszka Lekawa-Raus,† Andrzej Gruszczyk,‡ and Krzysztof K. K. Koziol*,†

†Department of Materials Science and Metallurgy, University of Cambridge, 27 Charles Babbage Road, CB3 0FS, Cambridge, U.K. and ‡Welding Department, Silesian University of Technology, Konarskiego 18a, 44-100 Gliwice, Poland

ABSTRACT Joining of carbon materials *via* soldering has not been possible up to now due to lack of wetting of carbons by metals at standard soldering temperatures. This issue has been a severely restricting factor for many potential electrical/electronic and mechanical applications of nanostructured and conventional carbon materials. Here we demonstrate the formation of alloys that enable soldering of these structures. By addition of several percent (2.5−5%) of transition metal such as chromium or nickel to a standard lead-free soldering tin based alloy we obtained a solder that can be applied using a commercial soldering iron at typical soldering temperatures of approximately 350 °C and at ambient conditions. The use of this solder enables the formation of mechanically strong and electrically conductive joints between carbon materials and, when supported by a simple two-step technique, can successfully bond carbon structures to any metal terminal. It has been shown using optical and scanning electron microscope images as well as X-ray diffraction patterns and energy dispersive X-ray mapping that the successful formation of carbon−solder bonds is possible, first, thanks to the uniform nonreactive dispersion of transition metals in the tin-based matrix. Further, during the soldering process, these free elements diffuse into the carbon−alloy border with no formation of brazing-like carbides, which would damage the surface of the carbon materials.

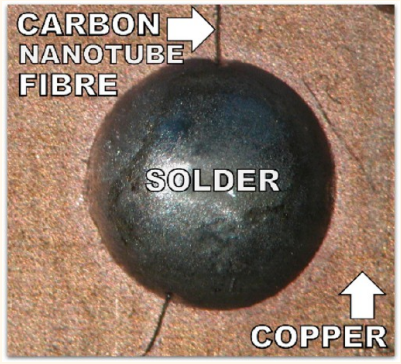

KEYWORDS: soldering alloys · wetting · carbon nanomaterials · carbon fibers

Unique properties of conventional and nanostructured carbon materials, including low-density, high-melting/sublimation temperature, high thermal and electrical conductivity, resistivity to corrosion and erosion, and great mechanical performance in a wide range of temperatures, could make them unrivaled candidates for an extremely wide range of applications.[1−8] As an example particular interest in such materials is from the transportation industry including aerospace, rail, and automotive engineering, where the low weight of plane, train, or car components is a significant fuel- and cost-saving factor. In these areas carbon materials could serve not only as recently introduced construction elements but also as functional coatings, sensors, or electrical, thermal, and optical systems. However, up to now the usage of carbon materials has been severely restricted in many applications due to a major difficulty of joining of these structures together or to other materials such as metals.[6,9,10]

The basic techniques that have been used up to now for joining of conventional carbon materials comprised (i) adhesive bonding,[11,12] (ii) mechanical joining,[12] and (iii) brazing.[11,13−15] Each of these techniques has been devised for specific purposes, and none of them can fulfill the requirements set for all potential applications.

Commonly used adhesives, epoxy resins, which are employed mainly for joining carbon fibers with each other and with other materials including metals, may be used in some mechanical applications. However, due to brittleness, they fail, *e.g.*, under high-impact loads.

Moreover, the highly insulating properties of resins exclude them from any electrical or thermal applications.

The thermally conductive joints need to be produced *via* mechanical joining or brazing. The former technique is a common method of connecting graphite and carbon−carbon composites, particularly to other materials and especially metals. In the case of electronic and electrical applications, mechanical joining due to the need for the use of connectors and terminals increases the mass and size of devices and is not

* Address correspondence to (M. Burda) mb849@cam.ac.uk, (K. Koziol) kk292@cam.ac.uk.

Received for review April 13, 2015 and accepted August 9, 2015.

Published online August 09, 2015
10.1021/acsnano.5b02176

technically practicable in the case of micro- and nanoelectronic systems.

As mentioned above, thermally conductive joints may also be produced *via* brazing, which is also suitable for the preparation of electrical connections. Brazing offers as well the best strength of carbon−carbon and carbon−metal joints by overcoming the fundamental problem of achieving wetting of carbon materials. These brazing alloys use base matrices such as copper or silver and reactive elements, *e.g.*, titanium, vanadium, or zirconium. The presence of the latter elements ensures wetting and joining of carbons by the formation of carbides at their interface. Unfortunately, brazing entails the use of very high temperatures that exceed the decomposition temperature of most materials used in electronic applications such as printed circuit boards and also may lead to the combustion of carbon materials, particularly nanostructured ones.

As may be inferred from the above, particularly problematic are electrical and electronic connections. These require very conductive, yet mechanically strong bonds, easy to apply at both at macro- and microscale using relatively low temperatures. When joining metals, this normally is obtained in a widely used, low-cost, and simple process of soldering. The use of this method, unfortunately, has not been possible up to now in the case of carbon materials[1−8] due to the lack of alloys that could potentially wet carbons at low temperatures.[9,10] Considering the fact that recently widely explored nanomaterials such as carbon nanotubes and graphene are expected to revolutionize the transport of electric/electronic signals and as a result almost all parts of current technology, the presented issue becomes a highly urgent one.

To address this burning problem, we developed new soldering alloys that for the first time ever enable low-temperature joining of various carbon materials including carbon fibers or carbon nanotube assemblies in both carbon−carbon and carbon−metal arrangements. The use of these carbon alloys allows fast formation of mechanically strong bonds that are electrically conductive, simultaneously. The soldering process itself is simple and inexpensive and can be easily applied under industrial conditions. Here, we present the design and analysis of properties of as-made alloys as well as show examples of the soldered bonds and their performance tests.

RESULTS AND DISCUSSION

Standard, commercially available, soldering alloys contain tin, copper, silver, lead, bismuth, indium, gallium, zinc, antimony, cadmium, germanium, gold, aluminum, and traces of other metals that due to their nonreactive nature and high surface tension do not wet carbon-based materials. On the basis of the example of brazing alloys, it can be expected that addition of a reactive component chosen from the transition metals group to a nonreactive low-melting-point base may improve wetting in carbon−metal systems, on the condition that the transition metal is highly active in a given matrix.

Assuming the wetting of a reactive nature as the main mechanism determining the effectiveness of the new soldering material, an alloy group in the SAC-X

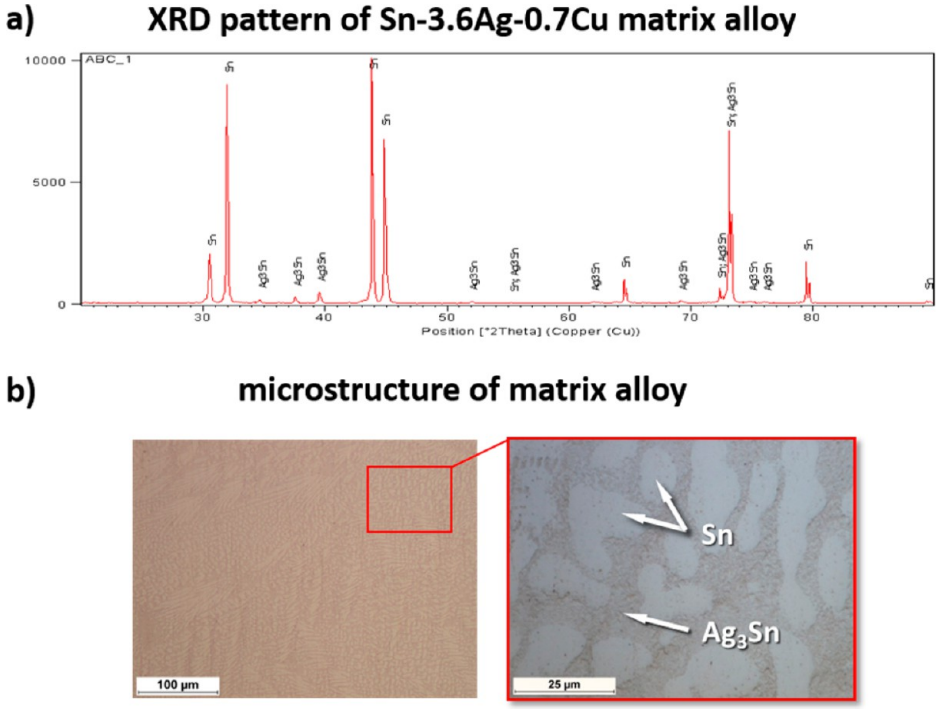

Figure 1. (a) X-ray diffraction pattern and (b) optical microscope images for Sn−3.6Ag−0.7Cu alloy.

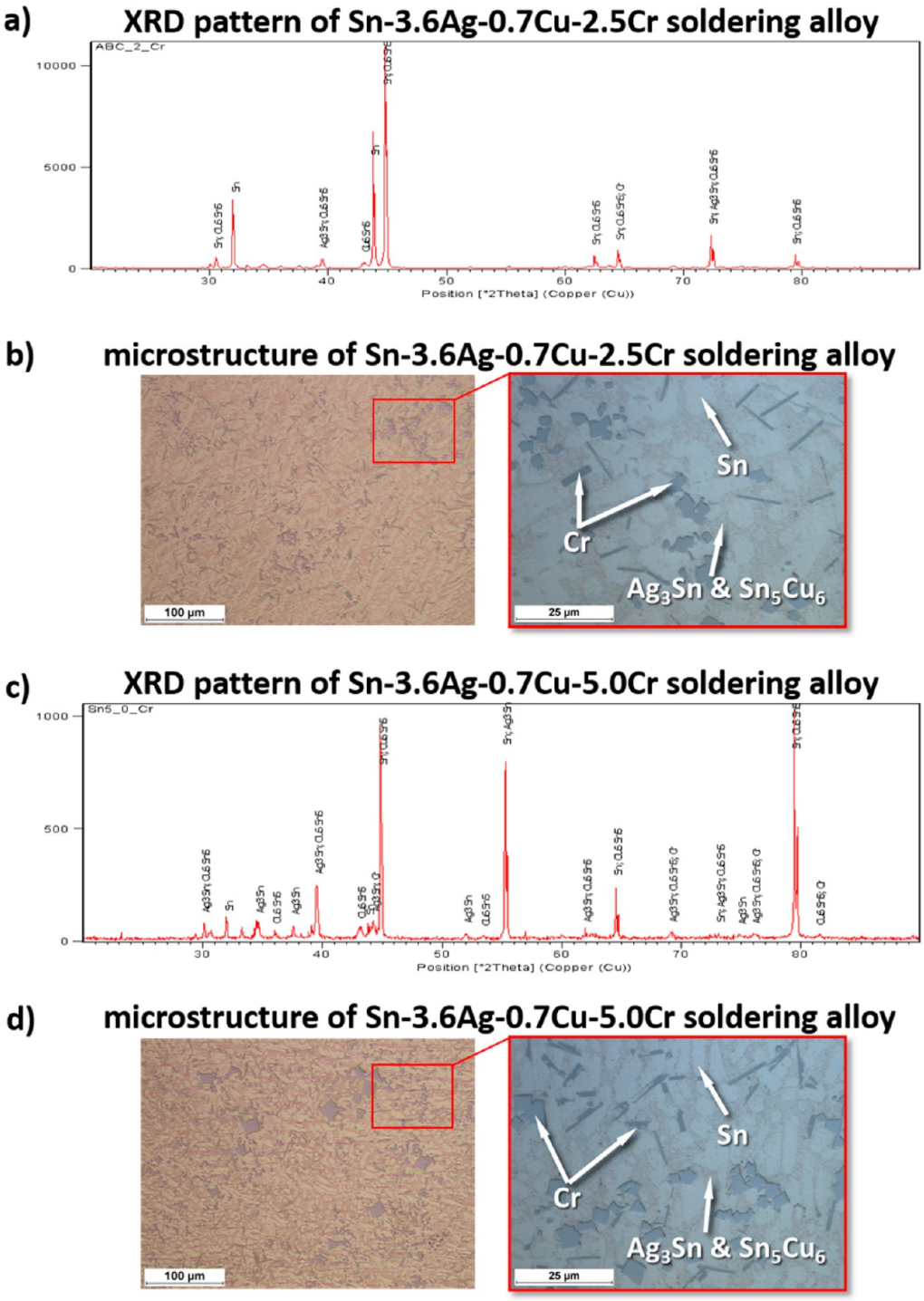

Figure 2. (a) X-ray diffraction pattern and (b) optical microscope images for Sn−3.6Ag−0.7Cu−2.5Cr and (c, d) Sn−3.6Ag−0.7Cu−5.0Cr.

arrangement was designed. SAC corresponds to near-eutectic Sn−3.6Ag−0.7Cu soldering alloy, currently considered as one of the best replacements for toxic lead-based soldering alloys. X constitutes active components chosen from the transition metals group, namely, Cr, Ti, and Ni, with concentrations of 2.5 and 5.0 wt %. The effect of adding a small amount of Cr, Ti, and Ni on the usability of SAC solders has been discussed in the literature.[16] However, so far, use of concentrations above 1 wt % has not been a subject of systematic research. Moreover, past research was focused on the influence of additives on the microstructure and physical or mechanical properties of SAC alloys without consideration of their applicability in soldering of carbon-based materials.

According to the Sn−Ag,[17] Sn−Cu,[18] and Ag−Cu[19] phase diagrams, a near eutectic Sn−3.6Ag−0.7Cu alloy should contain two intermetallic phases: Ag_3Sn and

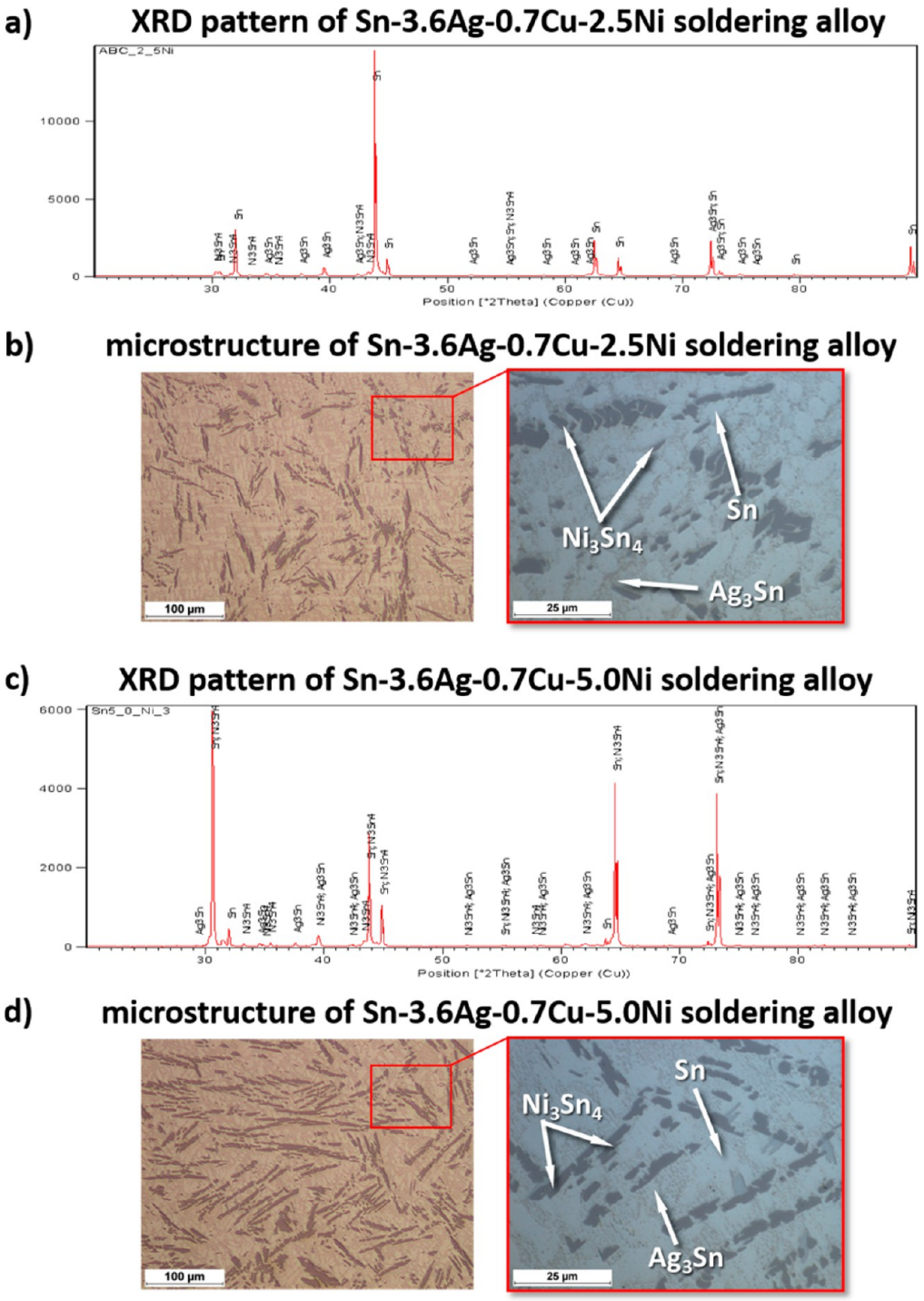

Figure 3. (a) X-ray diffraction pattern and (b) optical microscope images for Sn−3.6Ag−0.7Cu−2.5Ni and (c, d) Sn−3.6Ag−0.7Cu−5.0Ni.

Sn_5Cu_6, the first of which was indeed detected by X-ray diffraction (XRD) analysis made on the cross section of alloy ingots (Figure 1). The lack of Sn_5Cu_6 in the presented X-ray pattern probably resulted from the fact that the concentration of Cu was very low, *i.e.*, below 1%, and therefore made it difficult to identify using XRD.

Cr does not form intermetallic phases with Sn,[20] Ag,[21] and Cu,[22] and as a result X-ray analysis made on the cross section of quaternary Sn−3.6Ag−0.7Cu−2.5Cr and Sn−3.6Ag−0.7Cu−5.0Cr alloys revealed the presence of intermetallic phases related to the SnAgCu matrix (in this case both Ag_3Sn and Sn_5Cu_6) and pure Cr, which can be seen in the SAC matrix as uniformly distributed very fine regular grains (Figure 2).

Ni does not form any intermetallic phases with Ag[23] and Cu[24] but does with Sn.[25] Hence, Sn−3.6Ag−0.7Cu−2.5Ni and Sn−3.6Ag−0.7Cu−5.0Ni contain

Ag_3Sn as well as Ni_3Sn_4, which can be found in the Sn–Ni phase diagram (Figure 3).[25] Again, the low concentration of Cu probably resulted in the lack of Sn_5Cu_6 in the presented X-ray pattern.

Neither XRD nor optical and scanning electron microscopy analyses of SAC, SAC-Cr, and SAC-Ni alloys revealed the presence of compounds preventing the formation of usable solders such as carbides or ceramic contaminations, which could be produced during vacuum induction melting using ceramic crucibles. (The small peaks present in XRD patterns in Figures 2a and c, which were difficult to recognize and therefore were left unnamed, cannot be related to these compounds. Considering the fact that these are very small peaks, produced in different positions of the patterns depending on the test, they may be interpreted as trace impurities and, as will be seen further, are not harmful to the solders.) However, unlike Cr and Ni, Ti forms intermetallic compounds with all elements of a nonreactive matrix and simultaneously is reactive to ceramic materials. It was found that formation of metal–metalloid inclusions, due to reaction with Al_2O_3 crucibles, was highly detrimental to castability and formability of Ti-rich SAC alloys (Figure 4), and as a result further analysis of these alloys was abandoned.

SAC-Cr and SAC-Ni ingots, evaluated as free of contaminations as well as macro- and microsegregations, were further used for soldering of carbon fibers and carbon nanotube (CNT) fibers (*i.e.*, wire-like macroscopic assemblies of axially aligned carbon nanotubes[6,28,29]) to the copper layer of printed circuit boards. The examples of solders and joints prepared with the use of Sn–3.6Ag–0.7Cu–2.5Cr alloy and CNT fiber are presented in Figure 5.

According to the phase diagram, the melting range of as-made nonreactive Sn–3.6Ag–0.7Cu alloy is approximately 217–220 °C.[26] Addition of 2.5 and 5.0 wt % Cr to the near-eutectic SAC matrix does not change the solidus temperature but significantly increases the liquidus temperature, which, based on the equilibrium phase diagram, is ~950 and ~1050 °C, respectively.[20] In the case of SAC-Ni a high-melting additive increase the liquidus temperature to ~660 and ~730 °C for 2.5 and 5.0 wt %, respectively.[25] A wide pasty range (solidus–liquidus) enforces soldering using alloys in a semiliquid state and, due to the low flowing power just above the solidus temperature (220–300 °C), the soldering temperature in range 350–450 °C was found optimal.

A common difficulty in the processing of solders results from formation of oxides, which hinder movement of the triple line, *i.e.*, the spreadability of the solder (Figure 5a).

Therefore, the efficiency of low-, medium-, and high-activity fluxes was tested. The use of highly active fluxes, such as diluted orthophosphoric acid, improved the spreadability of Cr- and Ni-rich SAC alloys on a copper substrate, but simultaneously impaired interaction of the solder with carbon-based materials (Figure 5b). On the other hand, medium- and low-activity rosin-based or water-soluble fluxes did not affect the interaction between the solder and carbon material but concurrently were not efficient in improving the spreadability of the solder. Considering all the above and the fact that despite very weak interaction with the copper substrate, pure Cr- and Ni-rich alloys, due to their reactive nature, easily adhere to carbon materials, a two-step soldering method was devised.

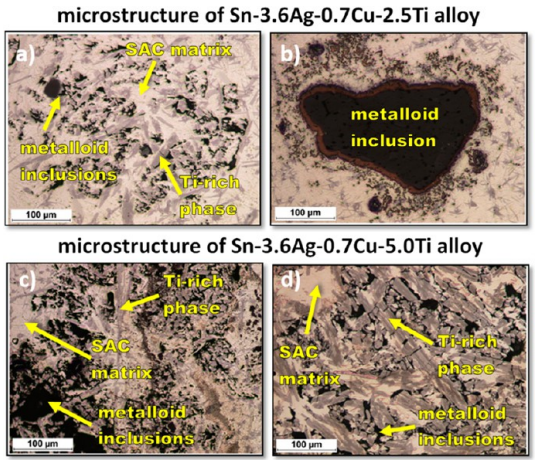

Figure 4. Optical microscope images showing typical metal–metalloid inclusions in microstructure of (a, b) Sn–3.6Ag–0.7Cu–2.5Ti and (c, d) Sn–3.6Ag–0.7Cu–5.0Ti alloys.

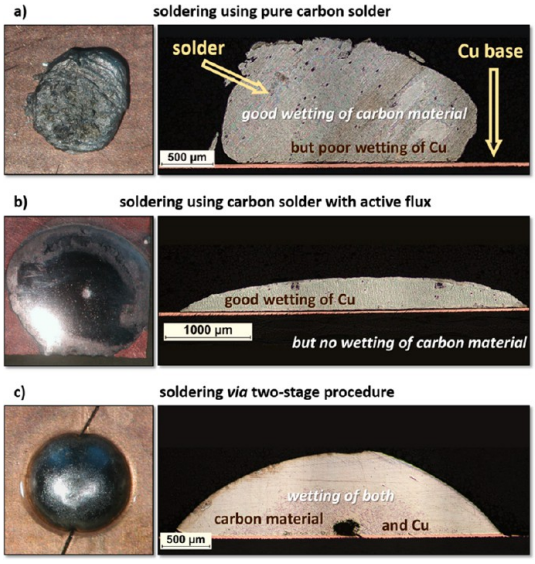

Figure 5. Images of the solders and their wetting angles on a Cu base obtained during soldering with the use of Sn–3.6Ag–0.7Cu–2.5Cr alloy: (a) without application of fluxes or buffer layers (clear nonwetting behavior toward Cu), (b) with the use of active fluxes (good wetting of Cu surface but no wetting of CNT fiber), (c) upon employment of a two-stage procedure (good wetting of both Cu surface and CNT fiber). Analogous results were obtained with the use of Sn–3.6Ag–0.7Cu–5.0Cr, Sn–3.6Ag–0.7Cu–2.5Ni, and Sn–3.6Ag–0.7Cu–5.0Ni alloys on both CNT and carbon fibers.

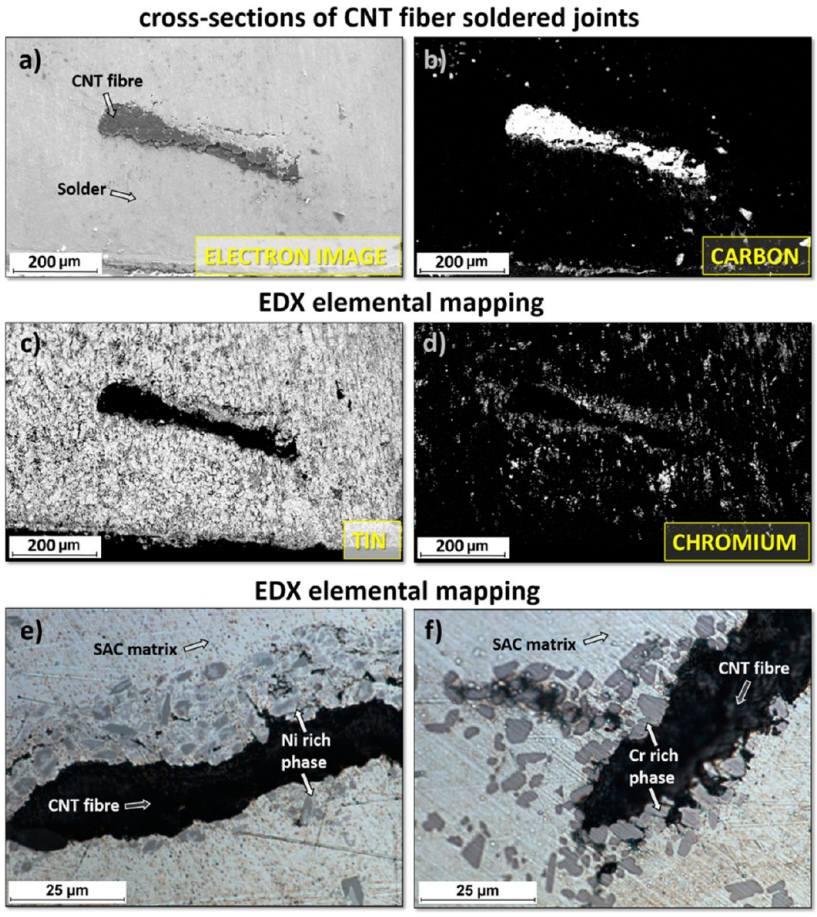

Figure 6. Cross sections of the soldered joints of carbon nanotube (CNT) fibers performed with the use of Sn−3.6Ag−0.7Cu−2.5Cr and Sn−3.6Ag−0.7Cu−2.5Ni. (a) Electron image and (b, c, d) maps of the distribution of chemical elements for a Cr-rich alloy. (e, f) Maps of the distribution of chemical elements showing a significant concentration of a Ni- and Cr-rich phase around the carbon nanotube fiber.

The two-step method takes into account formation of a buffer layer on the Cu substrate with the aid of any nonactive lead or lead-free solder. The Cr- or Ni-rich SAC alloy melted on the surface of the buffer layer, which has a lower liquidus temperature than the active solder, undergoes a transition into liquid state under the protective layer of the surrounding metal and as a result allows adhering to carbon materials while not becoming oxidized. Simultaneously, the nonactive or low-activity flux present in the commercially available solder wires enables the activation of the base and improves the spreadability of the molten solder mixture (Figure 5c).

The microscopic analysis and energy-dispersive X-ray (EDX) mapping at the cross section of solder joints made *via* two-stage soldering using SAC-Cr and SAC-Ni alloys showed a homogeneous distribution of Sn and other nonactive components and a significant concentration of chromium and nickel around the carbon nanotube fibers, which indicates intense diffusion of active components even at a relatively low temperature (see Figure 6 and Figure S1 in the Supporting Information). However, none of the analysis techniques showed any loss of carbon material or formation of new compounds on the surface of the fibers. This indicates that unlike brazing, this joining method is safe for nanostructured carbon materials.

Based on the two-step soldering procedure, a method of overlap joining of carbon nanotube fibers as well as their cords (many fibers bundled in parallel) was developed. The modified procedure was based on premetalization of CNT fibers using Cr- or Ni-rich SAC alloys followed by their spot heating, leading to formation of a joint (Figure 7). A series of joints of individual carbon nanotube fibers with a linear density varying from 0.4 to 0.8 tex (g km^{-1}) was made using Sn−3.6Ag−0.7Cu−2.5Cr/5.0 Cr and Sn−3.6Ag−0.7Cu−2.5Ni/5.0 Ni alloys.

The individual carbon nanotube fibers as well as their joints were subject to a static tensile test. All of the analyzed samples fractured within the fiber area, at an average tensile strength of 0.8 N tex^{-1}, which is a typical strength of the CNT fibers used. The lack of pull-out of the CNT fiber from the solder demonstrates strong interaction between the carbon nanotube fiber and the Cr- and Ni-rich SAC solder.

For comparative purposes, the same procedure was used to form overlapped joints of carbon fibers.

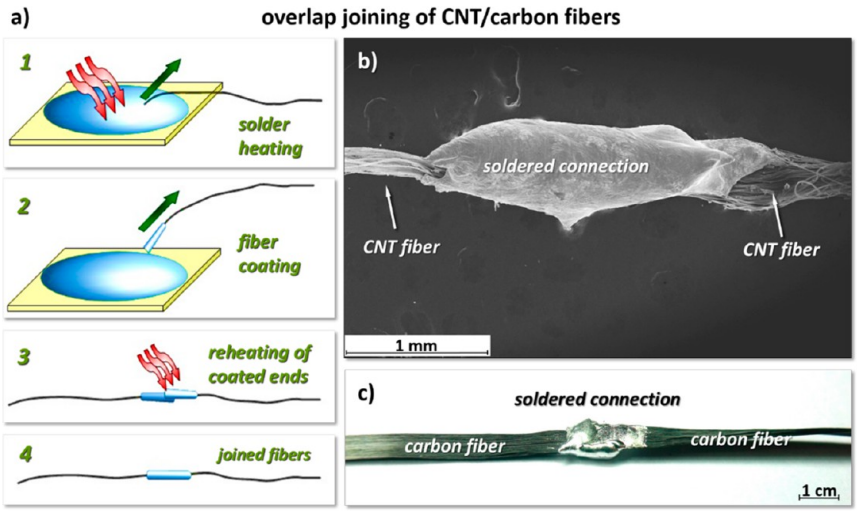

Figure 7. (a) Procedure of overlap joining of carbon/carbon nanotube fibers including the coating of the fibers with the metal layer and reheating of the coated fiber ends in order to obtain the connection. Images of two (b) carbon nanotube fiber cords and (c) tows of carbon fibers soldered together with the use of SAC-X (here Sn−3.6Ag−0.7Cu−2.5Cr) active alloy.

The tensile tests performed on the joints with a constant length of the overlap of 20 mm (Figure 7 f) showed that the joints made with SAC-Cr alloys can transfer up to as much as 20% of the maximum load of the tow of carbon fibers used (measured strength of the tow 2.4 GPa) and up to 10% for SAC-Ni alloys. There was no difference in strength observed for varying concentrations of Cr and Ni in the SAC-X alloys.

The electrical measurements performed on similar samples showed that the resistance of a 18 cm long continuous fiber tow amounts to 13.9 Ω, while the resistance of a tow with the same length but with a 2 cm overlapped joint in the middle soldered together equals 13.1 Ω. This indicates that the contact resistance of the soldered carbon fiber joint is negligible.

The quality of carbon nanotube fiber electrical connections was assessed by comparison with currently the best known laboratory connection method using commercial silver paint. The silver paint is a solution of silver nanoparticles in organic solvents due to which it easily infiltrates the interior of the CNT fibers, providing currently the lowest possible contact resistance, but a highly brittle joint. For comparison 4 pairs of similar 50 mm long fibers were connected on both ends using either silver paint or one of the SAC-X solders, *i.e.*, Sn−3.6Ag−0.7Cu−2.5Cr, Sn−3.6Ag−0.7Cu−5.0Cr, Sn−3.6Ag−0.7Cu−2.5Ni, or Sn−3.6Ag−0.7Cu−5.0Ni (Figure 8).

The resistance measured for Sn−3.6Ag−0.7Cu−2.5Cr and Sn−3.6Ag−0.7Cu−5.0Cr alloys was 2.5% and 3.9% higher than for silver paint joined counterparts, while the Sn−3.6Ag−0.7Cu−2.5Ni-joined fiber showed no significant change in resistance and Sn−3.6Ag−0.7Cu−5.0Ni showed an increase of 6.3%

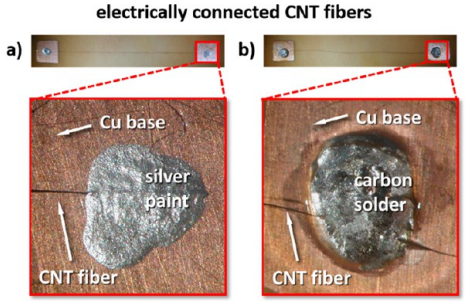

Figure 8. Joints made for resistance testing: (a) using silver conductive paint and (b) Sn−3.6Ag−0.7Cu−2.5Cr alloy.

as compared to silver-painted samples. This indicates that solders provide very good electrical connection to the CNT fibers although they do not infiltrate the interior, which is probably the reason for a small increase in resistance as compared to silver-painted fibers.

CONCLUSIONS

The presented results demonstrate the usefulness of Cr- and Ni-rich SAC alloys and the devised two-step soldering procedure for joining carbon nanotube based fibers and carbon fibers to each other or to any metal base that can be wetted by conventional commercially available soldering alloys. Soldering using Cr- and Ni-rich SAC alloys does not damage CNTs/carbon fibers, maintaining their intrinsic electrical and mechanical performance sufficient for most applications requiring the transport of electric signals. Moreover, fibers can be soldered using a standard soldering iron with no need for controlled atmosphere or high temperatures typical for reactive brazing, making the process simple, energy efficient, cost-effective, and industrially viable. Therefore, the presented new carbon-joining

technique may enable many new technologies and significant advancements in the existing industries particularly in such areas as aerospace and rail engineering.

METHODS

Preparation of Alloys. Transition metal rich SAC alloys were made using a Balzers VSG 02 vacuum induction furnace. Lumps of 99.97% Sn, 99.99% Ag, 99.9% Cu, and 99.9% pure Cr, Ti, and Ni were melted in 0.2 l Al_2O_3 crucibles under a controlled argon atmosphere at the pressure of 0.8 bar. Further, the melts were casted into 10 mm cold graphite molds. For comparative purposes a nonreactive Sn−3.6Ag−0.7Cu alloy was made using the same input materials and casting method.

Materials. Carbon nanotube fibers used for the experiments were manufactured *via* direct spinning from the floating catalyst chemical vapor deposition furnace. The details of the procedure were described earlier.[6,28,29]

Experiments requiring carbon fibers were performed with the use of standard commercial carbon fiber tow 12000 HexTow IM10.

Alloys for soldering were cold forged from ingots using swaging machines. Thus, 1.0 mm wires for hand soldering were formed.

Joining. Soldering was performed with the use of a standard, commercial, JBC TOOLS CD, ESD station of 75 W power and temperature range of 90−450 °C, equipped with a JBC-T245-A soldering iron. All the bonds were prepared in atmospheric conditions (ambient air, room temperature, atmospheric pressure).

The silver paint used for comparative electrical measurements is a commercial solution of silver nanoparticles in organic solvents (1-ethoxypropan-2-ol, acetone, ethanol, ethyl acetate).[30] All the electrical tests were performed after 24 h to allow enough time for drying of the paint.

Analysis of Alloy Composition. The X-ray diffraction patterns of the alloys were obtained with the aid of a Philips X'pert X-ray diffractometer equipped with a PW 3020 goniometer.

Elemental mapping of the alloys was performed using a JEOL 5800 LV scanning electron microscope (SEM) equipped with an ultrathin window EDX detector.

Electrical Testing. The resistance of joined carbon and carbon nanotube fibers was measured in a four-point probe arrangement using a dc ohmmeter of a Keithley2000 multimeter.

Tensile Testing. Static tensile tests of joined carbon nanotube fibers and bonds were performed in a Favimat machine (Tex Techno Instruments).[27] The gauge length was set to 40 mm, and the testing speed to 10 mm min^{-1}.

Tensile tests on soldered carbon fiber samples were performed with the use of a Hounsfield 5 kN tester. The gauge length was set to 50 mm and testing speed to 10% min^{-1}.

Conflict of Interest: The authors declare no competing financial interest.

Supporting Information Available: The Supporting Information is available free of charge on the ACS Publications website at DOI: 10.1021/acsnano.5b02176.

Microscopic analysis and EDX mapping of solder joints (PDF)

Acknowledgment. M.B. and A.G. would like to acknowledge the financial support from the Narodowe Centrum Nauki, Poland (project number ODW/6222-B/T02/2011/40 and DEC-2011/01/B/ST8/03863). A.L.-R. and K.K.K.K. thank the European Research Council (under the Seventh Framework Program FP7/2007-2013, ERC grant agreement no. 259061) for funding this research. A.L.-R. is also grateful to Trinity College, University of Cambridge, for a Coutts Trotter Studentship. K.K.K.K. thanks as well the Royal Society for further financial support.

REFERENCES AND NOTES

1. Pierson, H. O. *Handbook of Carbon, Graphite, Diamonds and Fullerenes: Properties, Processing and Applications*; William Andrew, Elsevier Inc.: USA, 1994.
2. Fitzer, E. *Carbon Fibres and Their Composites*; Springer: London, UK, 2011.
3. Jorio, A.; Dresselhaus, G.; Dresselhaus, M., Eds. *Carbon Nanotubes: Advanced Topics in the Synthesis, Structure, Properties and Applications*; Springer-Verlag: Berlin Heidelberg, Germany, 2008.
4. De Volder, M. F.; Tawfick, S. H.; Baughman, R. H.; Hart, A. J. Carbon Nanotubes: Present and Future Commercial Applications. *Science* **2013**, *339*, 535–539.
5. Lan, Y.; Wang, Y.; Ren, Z. F. Physics and Applications of Aligned Carbon Nanotubes. *Adv. Phys.* **2011**, *60*, 553–678.
6. Lekawa-Raus, A. E.; Patmore, J.; Kurzepa, L.; Bulmer, J.; Koziol, K. K. Electrical Properties of Carbon Nanotube Based Fibers and Their Future Use in Electrical Wiring. *Adv. Funct. Mater.* **2014**, *24*, 3661–3682.
7. Novoselov, K. S.; Falko, V. I.; Colombo, L.; Gellert, P. R.; Schwab, M. G.; Kim, K. A Roadmap for Graphene. *Nature* **2012**, *490*, 192–200.
8. Feng, L.; Xie, N.; Zhong, J. Carbon Nanofibers and Their Composites: A Review of Synthesizing, Properties and Applications. *Materials* **2014**, *7*, 3919–3945.
9. Deng, Y.; Pecht, M. G.; Swift, J. A.; Wallace, S. J. Carbon Fiber-Based Grid Array Interconnects. *IEEE Trans. Compon. Packag. Technol.* **2007**, *30*, 716–723.
10. White, J.; Simpson, A. H.; Shteinberg, A.; Mukasyan, A. S. Combustion Joining of Refractory Materials: Carbon−Carbon Composites. *J. Mater. Res.* **2008**, *23*, 160–169.
11. Salvo, M.; Casalegno, V.; Vitupier, Y.; Cornillon, L.; Pambaguian, L.; Ferraris, M. Study of Joining of Carbon/Carbon Composites for Ultrastable Structures. *J. Eur. Ceram. Soc.* **2010**, *30*, 1751–1759.
12. Kweon, J.-H.; Jung, J.-W.; Kim, T.-H.; Choi, J.-H.; Kim, D.-H. Failure of Carbon Composite-to-Aluminum Joints with Combined Mechanical Fastening and Adhesive Bonding. *Composite Structures* **2006**, *75*, 192–198.
13. Wu, W.; Hu, A.; Li, X.; Wei, J. Q.; Shu, Q.; Wang, K. L.; Yavuz, M.; Zhou, Y. N. Vacuum Brazing of Carbon Nanotube Bundles. *Mater. Lett.* **2008**, *62*, 4486–4488.
14. Xiong, J. H.; Huang, J. H.; Zhang, H.; Zhao, X. K. Brazing of Carbon Fiber reinforced SiC Composite and TC4 Using Ag−Cu−Ti Active Brazing Alloy. *Mater. Sci. Eng., A* **2010**, *527*, 1096–1101.
15. Ray, A. K.; Kar, A.; Kori, S. A.; Pathak, L. C.; Sonnad, A. N. Graphite-to-304SS Braze Joining by Active Metal-Brazing Technique: Improvement of Mechanical Properties. *J. Mater. Eng. Perform.* **2013**, *22*, 258–266.
16. Kotadia, H. R.; Howes, P. D.; Mannan, S. H. A review: On the Development of Low Melting Temperature Pb-Free Solders. *Microelectron. Reliab.* **2014**, *54*, 1253–1273.
17. Karakaya, I.; Thompson, W. T. The Ag-Sn (Silver-Tin) System. *Bull. Alloy Phase Diagrams* **1987**, *8*, 340–347.
18. Saunders, N.; Miodownik, A. P. The Cu-Sn (Copper-Tin) System. *Bull. Alloy Phase Diagrams* **1990**, *11*, 278–287.
19. Subramanian, P. R.; Perepezko, J. H. The Ag-Cu (Silver-Copper) System. *J. Phase Equilib.* **1993**, *14*, 62–72.
20. Venkatraman, M.; Neumann, J. P. The Cr−Sn (Chromium-Tin) System. *J. Phase Equilib.* **1988**, *2*, 159–162.
21. Venkatraman, M.; Neumann, J. P. The Ag-Cr (Silver-Chromium) System. *Bull. Alloy Phase Diagrams* **1990**, *11*, 263–265.
22. Chakrabarti, D. J.; Laughlin, D. E. The Cr-Cu (Chromium-Copper) System. *Bull. Alloy Phase Diagrams* **1984**, *5*, 59–68.
23. Singleton, M.; Nash, P. The Ag−Ni (Silver-Nickel) System. *J. Phase Equilib.* **1987**, *8*, 119–121.
24. Gupta, K. The Cu-Ni-Ti (Copper-Nickel-Titanium) System. *J. Phase Equilib.* **2002**, *23*, 541–547.
25. Okamoto, H. Ni-Sn (Nickel-Tin). *J. Phase Equilib. Diffus.* **2008**, *29*, 297–298.

26. Ma, H.; Suhling, J. A Review of Mechanical Properties of Lead-Free Solders for Electronic Packaging. *J. Mater. Sci.* **2009**, *44*, 1141–1158.
27. Information on Favimat - mechanical testing machine for fibres. http://www.textechno.com/index.php/en/news-mainmenu-53/1-general/70-automatic-testing-on-carbon-fibres, accessed Feb 2015.
28. Li, Y.-L.; Kinloch, I. A.; Windle, A. H. Direct Spinning of Carbon Nanotube Fibers from Chemical Vapor Deposition Synthesis. *Science* **2004**, *304*, 276–278.
29. Sundaram, R. M.; Koziol, K. K.; Windle, A. H. Continuous Direct Spinning of Fibers of Single-Walled Carbon Nanotubes with Metallic Chirality. *Adv. Mater.* **2011**, *23*, 5064–5068.
30. Information on silver paint provided by the manufacturer, http://www.electrolube.com/core/components/products/msds/044/044SCP.pdf, accessed Feb 2015.